Magnetic structure of noncentrosymmetric perovskites $PbVO_3$ and $BiCoO_3$

I. V. Solovyev*

National Institute for Materials Science,

1-2-1 Sengen, Tsukuba, Ibaraki 305-0047, Japan

(Dated: December 23, 2011)

Abstract

It is well known that if a crystal structure has no inversion symmetry, it may allow for Dzyaloshinskii-Moriya magnetic interactions, operating between different crystallographic unit cells, which in turn should lead to the formation of long-periodic spin-spiral structures. Such a behavior is anticipated for two simple perovskites $PbVO_3$ and $BiCoO_3$, crystallizing in the noncentrosymmetric tetragonal $P4mm$ structure. Nevertheless, we argue that in reality $PbVO_3$ and $BiCoO_3$ should behave very differently. Due to the fundamental Kramers degeneracy for the odd-electron systems, $PbVO_3$ has no single-ion anisotropy. Therefore, the ground state of $PbVO_3$ will be indeed the spin spiral with the period of about one hundred unit cells. However, the even-electron $BiCoO_3$ has a large single-ion anisotropy, which locks this system in the collinear easy-axis C-type antiferromagnetic ground state. Our theoretical analysis is based on the low-energy model, derived from the first-principles electronic structure calculations.

I. INTRODUCTION

Magnetic materials, crystallizing in the noncentrosymmetric structure, have attracted a great deal of attention. The lack of the inversion symmetry gives rise to the ferroelectric activity. If the latter property is combined with the magnetism, the system becomes multiferroic, which has many merits for the next generation of electronic devices: for example, one can control the magnetization by applying the electric field and vice versa. The canonical example of such materials is $BiFeO_3$, which possesses simultaneously high magnetic transition temperature (about 640 K) and high ferroelectric Curie temperature (about 1090 K).[1]

Recently fabricated $PbVO_3$ and $BiCoO_3$ belong to the same category. They crystallize in the noncentrosymmetric tetragonal $P4mm$ structure (Fig. 1).[2,3] $BiCoO_3$ is an antiferro-

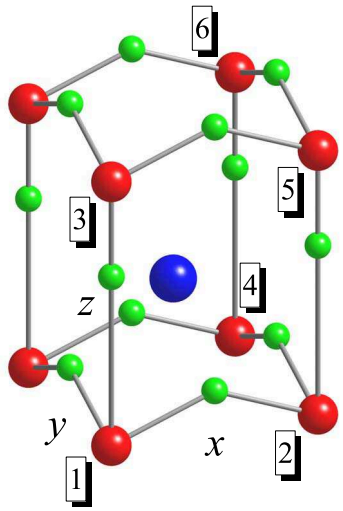

FIG. 1. (Color online) Fragment of the crystal structure of $BiCoO_3$. The Bi atoms are indicated by the big blue (dark) spheres, the Co atoms are indicated by the medium red (dark grey) spheres, and the oxygen atoms are indicated by the small green (light grey) spheres.

magnetic (AFM) insulator of the C-type with the Néel temperature of about 470 K.[3] The experimental information about $PbVO_3$ is rather controversial.[4,5] The magnetic susceptibility has a broad maximum around 200, which might be the sign of the antiferromagnetism. On the other hand, no long-range magnetic order was found down to 1.8 K in the neutron diffraction experiments. However, the analysis of the neutron data depends on the model of

the magnetic structure, which is typically assumed in the process of interpretation. Finally, the experimental studies of $PbVO_3$ were hampered by possible defects in the sample.[5]

According to first-principles electronic structure calculations, both $PbVO_3$ and $BiCoO_3$ are expected to have the C-type AFM ground state, although in $PbVO_3$ it is nearly degenerate with the G-type AFM state.[6,7] Giant electric polarization (more than 150 $\mu C/cm^2$) was predicted theoretically both for $PbVO_3$ and $BiCoO_3$,[6] which spurred additional interest to these systems.

Nevertheless, the violation of the inversion symmetry gives rise to a number of interesting effects, which are not currently accessible by the first-principles electronic structure calculations, simply due to their complexity. One of them is a complex magnetic ordering, caused by antisymmetric Dzyaloshinskii-Moriya interactions: in the noncentrosymmetric systems, these interactions, of the relativistic origin, can operate between different crystallographic unit cells, thus driving the formation of long-periodic spin-spiral superstructures.[8] Particularly, the idea of the spin-spiral order in various oxide materials has attracted much attention recently in the context of their multiferroic behavior and was proposed as one of the possible origins of such behavior.[9]

In this paper we will address some basic issues of the formation of the spin-spiral states in $PbVO_3$ and $BiCoO_3$. We will argue that, despite similarities in the lattice distortion and population of the crystal-field levels, these two compounds will behave very differently. Particularly, we will show that the long-periodic spin spiral is a probable candidate for the magnetic ground state of $PbVO_3$, where due to the fundamental Kramers degeneracy, the single-ion anisotropy does not exists. On the contrary, the spin-spiral state in $BiCoO_3$ (for which the Kramers theorem is no longer applicable) is suppressed by the single-ion anisotropy, which reinforces the formation of the easy-axis collinear C-type AFM ground state. Our analysis is based on the low-energy model, derived from the first-principles electronic structure calculations. In this sense, this is the continuation of our previous works, devoted to 'realistic modeling' of complex oxide materials and other strongly correlated systems.[10–12]

The rest of the paper is organized as follows. In Sec. II we briefly discuss the construction of the low-energy model (in our case – the multiorbital Hubbard model) on the basis of first-principles electronic structure calculations. All model parameters can be found in the supplemental materials.[13] Sec. III A is devoted to semi-quantitative analysis of the spin

model, which can be derived from the multiorbital Hubbard model. Particularly, we consider the formation of incommensurate spin-spiral states, resulting from the competition of the isotropic exchange and Dzyaloshinskii-Moriya interactions, and explain the main difference in the behavior of the single-ion anisotropy in $PbVO_3$ and $BiCoO_3$. In Sec. III B, we will present results of extensive Hartree-Fock calculations for the long-periodic spin-spiral states in the electronic Hubbard model. Finally, in Sec. IV we will briefly summarize the main results.

II. CONSTRUCTION OF THE LOW-ENERGY MODEL

The magnetic properties of $PbVO_3$ and $BiCoO_3$ are mainly determined by the behavior of $3d$-bands located near the Fermi level. Therefore, our basic idea of our approach is to construct an effective low-energy model, formulated in the Wannier-basis for the $3d$-bands, and to solve it by using model techniques. More specifically, we adopt the form of the multiorbital Hubbard model on the lattice of transition-metal sites:

$$\hat{\mathcal{H}} = \sum_{ij} \sum_{\alpha\alpha'} t_{ij}^{\alpha\alpha'} \hat{c}_{i\alpha}^{\dagger} \hat{c}_{j\alpha'} + \frac{1}{2} \sum_{i} \sum_{\{\alpha\}} U_{\alpha\alpha'\alpha''\alpha'''} \hat{c}_{i\alpha}^{\dagger} \hat{c}_{i\alpha''}^{\dagger} \hat{c}_{i\alpha'} \hat{c}_{i\alpha'''}. \quad (1)$$

where we use the shorthand notations, according to which each Greek symbol stand for the combination of spin (s= $\uparrow$ or $\downarrow$) and orbital (m= xy, yz, $3z^2-r^2$, zx, or x^2-y^2) indices. All parameters of the model Hamiltonian can be derived in an *ab initio* fashion, on the basis of first-principles electronic structure calculations. For instance, the one-electron part $t_{ij}^{\alpha\alpha'}$ was obtained by using the downfolding procedure, and the Coulomb (and exchange) interactions $U_{\alpha\alpha'\alpha''\alpha'''}$ – by combining the constrained density-functional theory (DFT) with the random-phase approximation (RPA). The method was discussed in the literature, and for details the reader is referred to Ref. 10. Resent applications to multiferroic compounds can be found in Refs. 11 and 12. In all calculations we use experimental parameters of the crystal structure, reported in Refs. 2 and 3.

Without spin-orbit interaction, $t_{ij}^{\alpha\alpha'}$ is diagonal with respect to the spin indices $t_{ij}^{\alpha\alpha'} \equiv t_{ij}^{mm'}\delta_{ss'}$. The site-diagonal part of $\hat{t}_{ij} = \|t_{ij}^{mm'}\|$ describes the crystal-field effects, while the off-diagonal part stands for transfer integrals.

The crystal field stabilizes the xy orbitals (Fig. 2). The splitting between xy- and the following after them yz- and zx-orbitals is about 1 eV, both for $PbVO_3$ and $BiCoO_3$. The

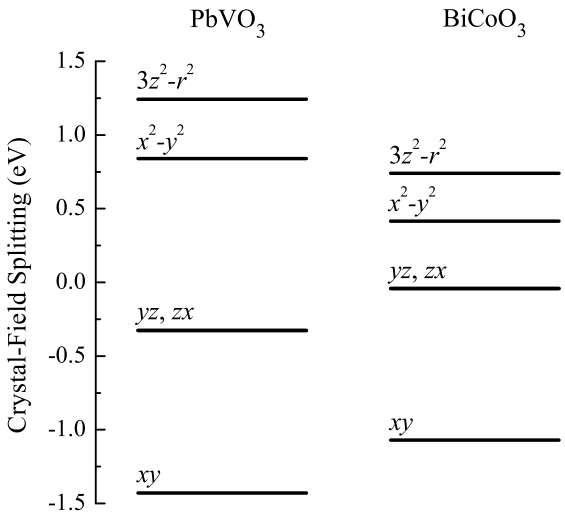

FIG. 2. Scheme of the crystal-field splitting in $PbVO_3$ (left) and $BiCoO_3$ (right).

x^2-y^2 and $3z^2-r^2$ orbitals lie in the higher-energy region (and are substantially higher for $PbVO_3$, in comparison with $BiCoO_3$). Thus, from the viewpoint of the crystal-field splitting, $PbVO_3$ and $BiCoO_3$ are expected to be very similar: $PbVO_3$ has only one d-electron, which will occupy the xy orbital. Amount six d-electrons of $BiCoO_3$, the one for the minority-spin states will also occupy the xy orbital and interact with the spherical d-electron density of occupied majority-spin shell.

The details of transfer integrals can be found in Ref. 13. One of the most interesting features in $\hat{t}_{ij}$ is the appearance of the so-called 'forbidden hoppings', for example between $3z^2-r^2$ and zx orbitals in the bond 1-2, which would not exist in the centrosymmetric structure (see Fig. 1 for the notations of atomic sites). These transfer integrals have the following form (in meV):

$$\hat{t}_{12} = \begin{pmatrix} -173 & 38 & 0 & 0 & 0 \\ -38 & 44 & 0 & 0 & 0 \\ 0 & 0 & 50 & -116 & 2 \\ 0 & 0 & 116 & 196 & -321 \\ 0 & 0 & 2 & 321 & -262 \end{pmatrix}$$

and

$$\hat{t}_{12} = \begin{pmatrix} -56 & 6 & 0 & 0 & 0 \\ -6 & 38 & 0 & 0 & 0 \\ 0 & 0 & 34 & -48 & -3 \\ 0 & 0 & 48 & 231 & -228 \\ 0 & 0 & -3 & 228 & -164 \end{pmatrix},$$

for $PbVO_3$ and $BiCoO_3$, respectively, in the basis of xy, yz, $3z^2-r^2$, zx, and x^2-y^2 orbitals. The microscopic origin of such forbidden hoppings was considered in Ref. 10: due to the parity violation, the Wannier orbital, which is formally labeled as "$3z^2-r^2$" has some weight of the p_z orbitals and, therefore, can interact with the zx orbitals of the neighboring sites. Such hoppings give rise to the antisymmetric part of $\hat{t}_{ij}$, which is responsible for the appearance of Dzyaloshinskii-Moriya interactions. Similar situation takes place in the bonds 1-4 and 1-5. On the contrary, due to the rotational symmetry, the transfer integrals in the bond 1-3 are diagonal with respect to the orbital indices (the actual values are $t_{13}^{mm}= -45$, 4, -237, 4, and -21 meV for $PbVO_3$, and $t_{13}^{mm}= -19$, 24, -42, 24, and -34 meV for $BiCoO_3$ – other details can be found in Ref. 13). Therefore, the 'forbidden hoppings' do not take place and Dzyaloshinskii-Moriya interactions will vanish.

For the relativistic spin-orbit interaction (SOI), we adopt two schemes. In the first one, we evaluate SOI only at the transition-metal sites and add it to the site-diagonal part of $t_{ij}^{\alpha\alpha'}$ in the form $\xi\mathbf{LS}$, where $\xi= 35$ and 81 meV for $PbVO_3$ and $BiCoO_3$, respectively. Thus, the effects of the SOI are expected to be larger in $BiCoO_3$: due to large ξ and smaller crystal-field splitting (Fig. 2), which competes with SOI. If it is not specified otherwise, we will refer to this scheme, for which most of the calculations have been performed. Nevertheless, as a test, we use also the second scheme, where SOI was included at all atoms on the level of the band-structure calculations and then corresponding parameters $t_{ij}^{\alpha\alpha'}$ were derived through the downfolding procedure. For example, this schemes takes into account the effect of large SOI at heavy atoms Pb and Bi.

The spin-dependence of Coulomb matrix elements has the standard form: $U_{\alpha\alpha'\alpha''\alpha'''}= U_{mm'm''m'''}\delta_{ss'}\delta_{s''s'''}$. The details of $U_{mm'm''m'''}$ can be found in Ref. 13. Rough idea about the strength of the matrix elements $U_{mm'm''m'''}$ can be obtained by interpolating them in terms of three characteristic averaged parameters U, J and B, which would take place in the centrosymmetrical environment of isolated atoms. In these notations, $U = F^0$ is the

on-site Coulomb interaction, $J = (F^2 + F^4)/14$ is the intraatomic exchange interaction, and $B = (9F^2 - 5F^4)/441$ is the 'nonsphericity', in terms of radial Slater's integrals F^0, F^2 and F^4. In the other words, U enforce the charge stability of certain atomic configurations, while J and B are responsible for the Hund rules. The results of such interpolation are shown in Table I. One can clearly see that the on-site Coulomb repulsion U is strongly

TABLE I. Averaged values of the Coulomb interaction U, exchange interaction J, and the nonsphericity B, obtained from the fitting of the matrix elements $U_{mm'm''m'''}$. All parameters are measured in electron volt.

compound	U	J	B
$PbVO_3$	1.57	0.84	0.08
$BiCoO_3$	2.38	0.90	0.09

screened, especially in $PbVO_3$, while other parameters are close to atomic values. We use this interpolation only for explanatory purposes, while all practical calculations were performed with actual parameters $U_{mm'm''m'''}$ reported in Ref. 13. The deviation of $U_{mm'm''m'''}$ from the centrosymmetric form is quite strong. For example, in the case of $BiCoO_3$, the diagonal matrix elements vary as U_{mmmm}= 3.84, 3.39, 2.94, 3.39, and 3.48 eV for m= xy, yz, $3z^2-r^2$, zx, and x^2-y^2, respectively.

After the construction, the model (1) is solved in the Hartree-Fock (HF) approximation.[10]

III. RESULTS AND DISCUSSIONS

A. Qualitative analysis based on the spin Hamiltonian

The existence of the spin-spiral states in noncentrosymmetric perovskites can be understood in the framework of the spin model:[14]

$$\hat{\mathcal{H}}_S = -\sum_{\langle ij \rangle} J_{ij} \boldsymbol{S}_i \boldsymbol{S}_j + \sum_{\langle ij \rangle} \mathbf{d}_{ij} [\boldsymbol{S}_i \times \boldsymbol{S}_j] + \sum_i \boldsymbol{S}_i \hat{\tau}_{ii} \boldsymbol{S}_i \tag{2}$$

(where J_{ij} is the isotropic exchange interaction, $\mathbf{d}_{ij}$ is the vector of antisymmetric Dzyaloshinskii-Moriya interactions, and $\hat{\tau}_{ii}$ is the single-ion anisotropy tensor), which can be obtained by mapping the electronic model (1) onto the spin one and integrating out all degrees of freedoms but spins. There are several ways how to do it. One possibility is to consider the

perturbation-theory expansion with respect to the infinitesimal spin rotations and SOI near the nonrelativistic ground state in the Hartree-Fock approximation.[15] In the following, the results of such model will be denoted by the symbols 'inf'. Moreover, for the d^1 configuration of $PbVO_3$ one can easily consider the theory of superexchange interactions in the second order with respect to the transfer integrals (in the following denoted by the symbol 'set').[16]

Then, neglecting for a while the single-ion anisotropy term, the energy of (classical) spin spiral in the zx-plane,

$$\langle \boldsymbol{S}_i \rangle = S\left(\sin \mathbf{q}\mathbf{R}_i, 0, \cos \mathbf{q}\mathbf{R}_i\right)$$

($\mathbf{R}_i$ being the radius-vector of the site i), is given by

$$E(\mathbf{q}) = -\sum_i \left(J_{0i} \cos \mathbf{q}\mathbf{R}_i - d^y_{0i} \sin \mathbf{q}\mathbf{R}_i\right),$$

and the spin-spiral vector $\mathbf{q} = (q_x, \pi, 0)$ in the ground state should correspond to the minimum of $E(\mathbf{q})$. Obviously, the isotropic exchange interactions (J_{0i}) will tend to establish a collinear spin structure with $\mathbf{q}\mathbf{R}_i = 0$ or π, while Dzyaloshinskii-Moriya interactions (d^y_{0i}) will deform this structure and make it incommensurate.[14] The Dzyaloshinskii-Moriya interactions are also responsible for the asymmetry between right-handed ($q_x > 0$) and left-handed ($q_x < 0$) spin-spiral states, which is manifested in the inequality $E(\mathbf{q}) \neq E(-\mathbf{q})$.

Parameters of isotropic exchange interactions (J_{ij}) are listed in Table II. We note that

TABLE II. Isotropic Heisenberg interactions (measured in meV) for $PbVO_3$ and $BiCoO_3$. Notations of the atomic sites are explained in Fig. 1. Results of the superexchange theory are denoted by the symbols 'set'. Results for infinitesimal spin rotations near the nonrelativistic ground state are denoted by the symbols 'inf'.

bond	$PbVO_3$ (set)	$PbVO_3$ (inf)	$BiCoO_3$ (inf)
1-2	−49.86	−44.71	−9.65
1-3	−3.63	−0.64	−0.15
1-4	4.76	3.20	−0.91
1-5	3.94	1.25	−1.19
1-6	3.61	1.25	−0.07

the schemes 'set' and 'inf' in the case of $PbVO_3$ provide very similar results. This seems to

be reasonable, because if the orbital configuration is quenched by the crystal-field splitting, the spin model (2) is well defined and the parameters are not sensitive to the way how they are defined (of course, provided that $|\hat{t}_{ij}/U| << 1$ and the schemes '*set*' makes a sense). The magnetic transition temperature, evaluated in the random-phase approximation (see Ref. 16 for details) for the G- and C-type AFM states, is of the order of 200 and 600 K for $PbVO_3$ and $BiCoO_3$, respectively. The experimental Néel temperature for $BiCoO_3$ is 470 K.[3] The situation in $PbVO_3$ is rather controversial. On the one hand, the results of the neutron powder diffraction experiment are not conclusive, because their interpretation strongly depends on the magnetic structure, which was *assumed* for the analysis of experimental data.[4] On the other hand, the magnetic susceptibility of $PbVO_3$ does display a broad maximum at around 200 K, which could be regarded as the sign of an antiferromagnetism. Moreover, the G-type antiferromagnetic order was proposed for the thin films of $PbVO_3$ below 130 K.[17]

Parameters of Dzyaloshinskii-Moriya interactions are shown in Table III. They are at least one order of magnitude smaller than J_{ij} for the same bonds.

TABLE III. Nonvanishing parameters of Dzyaloshinskii-Moriya interactions $\mathbf{d}_{ij} = (d^x_{ij}, d^y_{ij}, d^z_{ij})$ (measured in meV) for $PbVO_3$ and $BiCoO_3$. Notations of atomic sites are explained in Fig. 1. Other parameters are equal to zero. Results of the superexchange model are denoted by the symbols '*set*'. Results for infinitesimal spin rotations near the nonrelativistic ground state are denoted by the symbols '*inf*'. Note that Dzyaloshinskii-Moriya interactions vanish in the bond 1-3 due to symmetry constraints.

parameters	$PbVO_3$ (*set*)	$PbVO_3$ (*inf*)	$BiCoO_3$ (*inf*)
d^y_{12}	−0.98	−0.77	−0.13
$d^y_{14} = -d^x_{14}$	0.39	0.17	0
d^y_{15}	−0.11	−0.04	0
$d^y_{16} = -d^x_{16}$	−0.01	−0.03	0

Using these parameters, the spin-spiral vector q_x, can be estimated as $q_x a = \pi - \Delta\phi$ (a being the lattice parameter in the xy-plane), where $\Delta\phi = 6 \times 10^3\pi$ and $4 \times 10^3\pi$ for $PbVO_3$ and $BiCoO_3$, respectively. Thus, by considering only J_{ij} and $\mathbf{d}_{ij}$, both materials are expected to form spin-spiral structures, involving more than one hundred unit cells. As we will see below, this scenario indeed holds for $PbVO_3$, but not for $BiCoO_3$.

The main difference between $PbVO_3$ and $BiCoO_3$ is in the behavior of the single-ion anisotropy $\hat{\tau}_{ii}$. For the $S = 1/2$ compound $PbVO_3$, $\hat{\tau}_{ii}$ is expected to be zero as the consequence of fundamental Kramers degeneracy for the odd-electron systems. Particularly, the ground state of the self-interaction free ion V^{4+} is the Kramers doublet. Therefore, the rotation of spin corresponds to the unitary transformation of the wave function within this doublet without any energy cost. The situation is completely different for the $S = 2$ (or even-electron) compound $BiCoO_3$: the Kramers theorem is no longer valid, which formally allows for the finite $\hat{\tau}_{ii}$. This statement can be verified by direct calculations of the anisotropy energies $\Delta E = E_{\parallel} - E_{\perp}$ (where the symbols "$\parallel$" and "$\perp$" correspond to the spin configurations, where $\langle \boldsymbol{S}_i \rangle$ is parallel and perpendicular to the tetragonal z-axis). In the C-type AFM state, it yields ΔE= 0.02 and -5.63 meV per formula unit for $PbVO_3$ and $BiCoO_3$, respectively. Moreover, the main contribution to ΔE indeed originates from the single-ion anisotropy. This can be seen by repeating the same calculations in the atomic limit (and enforcing $\hat{t}_{ij}$=0 for all $i \neq j$), which yields ΔE= 0 and -5.86 meV per formula unit for $PbVO_3$ and $BiCoO_3$, respectively. Small deviations from the atomic limit are due to intersite ($i \neq j$) anisotropic interactions $\hat{\tau}_{ij}$, which can be evaluated in the '*set*'-model and are at least one order of magnitude smaller than $\mathbf{d}_{ij}$.[16] Using the obtained values of ΔE and the symmetry considerations, nonvanishing parameters of the single-ion anisotropy for $BiCoO_3$ can be estimated as $\tau_{ii}^{xx} = \tau_{ii}^{yy} = -\frac{1}{2}\tau_{ii}^{zz} = 0.49$ meV. Thus, we are dealing the following hierarchy of magnetic interactions $|J_{ij}| >> |\hat{\tau}_{ij}| >> |\mathbf{d}_{ij}|$. It means that the formation of the spin-spiral state in $BiCoO_3$ is strongly affected by the single-ion anisotropies, which will tend to restore the collinear spin structure by aligning the magnetic moments either parallel or antiparallel to the z-axis. Of course, the final answer about the from of the magnetic ground state of $BiCoO_3$ can be obtained only on the basis of detailed calculations, which we will discuss in the next section.

B. Solution of electronic model

In this section we present results of extensive Hartree-Fock calculations for large supercells, which allow for the spin-spiral solutions with $q_x a = \pi(|L| - 1)/L$, where $|L|$ is the number of cells along the x-axis: $L > 0$ and < 0 corresponds to the right- and left-handed alignment, respectively, and the limit $|L| \to \infty$ corresponds to the collinear C-type AFM

state. The main results are summarized in Figs. 3 and 4. One can clearly see that there

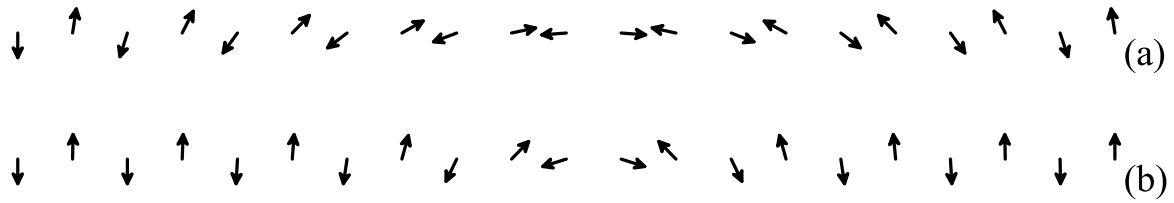

FIG. 3. Spin magnetic structure along the x-directions in the case of $PbVO_3$ (a) and $BiCoO_3$ (b), as obtained in the Hartree-Fock calculations for L= 21. Here, x is the horizontal axis and z is the vertical one.

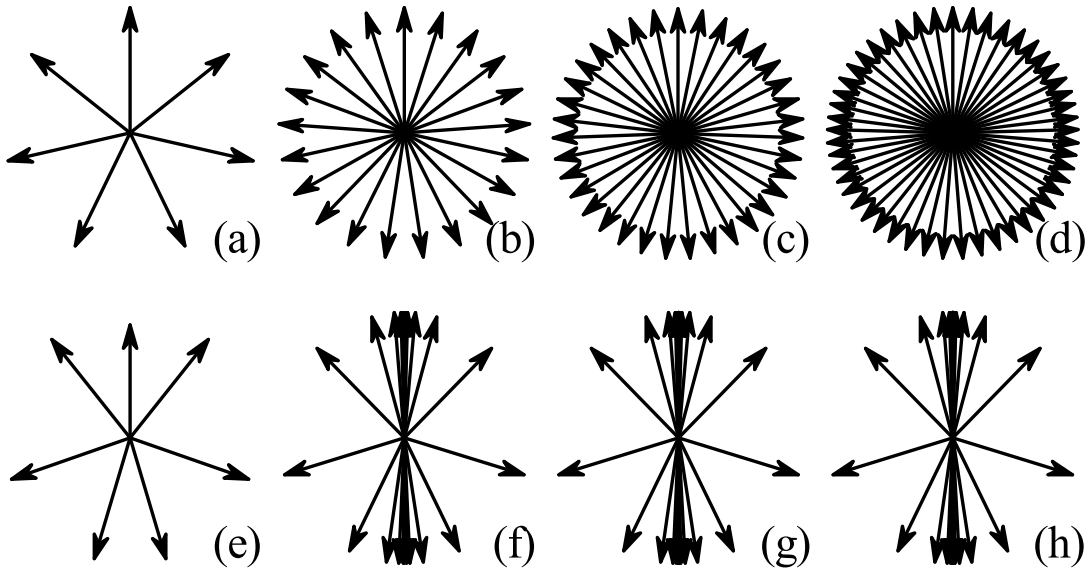

FIG. 4. Distribution of the spin magnetic moments (as if they were brought to the same origin) in the xz-plane of $PbVO_3$ (top) and $BiCoO_3$ (bottom): results of Hartree-Fock calculations for L= 7 ('a' and 'e'), 21 ('b' and 'f'), 35 ('c' and 'g'), and 49 ('d' and 'h'). Here, x is the horizontal axis and z is the vertical one.

is a big difference between $PbVO_3$ and $BiCoO_3$. $PbVO_3$ tends to form a homogeneous spin-spiral state, where the angle between neighboring magnetic moments along the x-axis remains constant (small deviations are caused by weak inter-site anisotropy effects). On the contrary, due to the large single-ion anisotropy, the spin-spiral configurations in $BiCoO_3$

are strongly distorted, and the moments are bunched around the z-axis (Figs. 4f-h). The so-called 'bunching effect' is well know for magnetic rare-earth metals and was intensively discussed already more than forty earth ago.[18] Thus, $BiCoO_3$ tends to form an inhomogeneous magnetic state, which corresponds to the (nearly) collinear AFM alignment in the wide part of the supercell, except small 'domain wall', where the spins undergo the reorientation within the area of about ten unit cells. The latter solutions were obtained for odd numbers of cells L, which in the AFM lattice results in the formation of the domain wall defect. For even L, the Hartree-Fock equations converge to the C-type AFM state. The spin pattern in the domain wall is well reproduced already for $L = 21$ (Fig. 4). For larger cells, the additional spins participate in the formation of the AFM regions, and are either parallel or antiparallel to the z-axis, leading to tiny changes in Figs. 4f-h, which are practically not distinguishable to the eye.

Results of total energy calculations (Fig. 5) are well consistent with the above finding. As expected for the spin-spiral states, the dependence of the total energy on $1/L$ in the case of $PbVO_3$ is well described by the parabola. Due to the Dzyaloshinskii-Moriya interactions, there is a small asymmetry of the total energy with respect to the inversion $L \to -L$ of chirality of the spin spiral. Thus, the total energy minimum, obtained from the extrapolation, corresponds to the spin-spiral ground state with $L \approx 94$. On the contrary, the total energy of $BiCoO_3$ is a linear function of $1/L$. This is because of the localized character of the domain wall, for which the total energy (divided by the total number of cells) is expected to scale as $1/L$. Thus, the minimum corresponds to the collinear C-type AFM ground state ($|L| \to \infty$), in which the total energy exhibits the derivative discontinuity. Nevertheless, even in this case, the total energy has different slops in the regions $L > 0$ and $L < 0$, again, due to the difference between the right- and left-handed spin-spiral alignment in the domain wall.

The crucial role of the single-ion anisotropy in the formation of the easy-axis C-type AFM ground state can be illustrated by repeating supercell calculations for $BiCoO_3$ with the same parameters of the model Hamiltonian, but with different number of valence electrons: one instead of six. Thus, according to the Kramers theorem, the single-ion anisotropy should vanish, similar to $PbVO_3$. The results for $L = 21$ are shown in Fig. 6, in comparison with regular $BiCoO_3$, including all six valence electrons. There are two effects. First, as was already discussed in Sec. II, the effects of SOI are generally larger in $BiCoO_3$, in

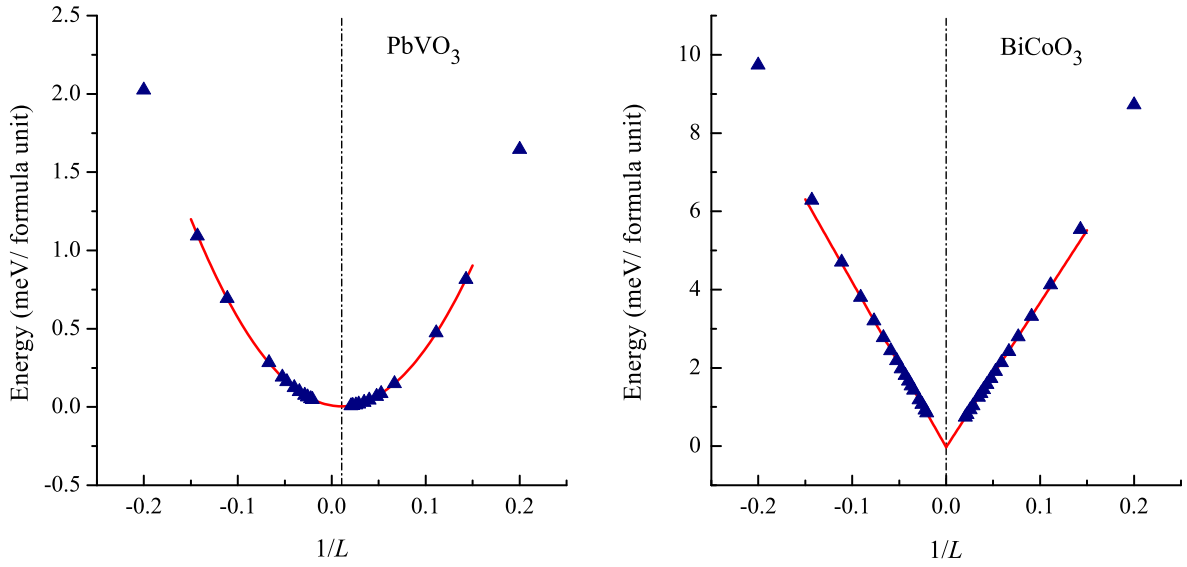

FIG. 5. (Color online) Total energies versus $1/L$ as obtained in the Hartree-Fock approximation for $PbVO_3$ (left) and $BiCoO_3$ (right). Calculated points are denoted by symbols. Solid line is the results of interpolation $E = a/L + b/L^2$ in the case of $PbVO_3$ (where $a = -0.99$ meV and $b = 46.36$ meV) and $E = a/L$ in the case of $BiCoO_3$ (where $a = -42.22$ meV for $L < 0$ and $a = 36.94$ meV for $L > 0$). The location of the total energy minimum is shown by the dot-dashed line.

comparison with $PbVO_3$. Therefore, inter-site anisotropic interactions become stronger, which is reflected in some bunching of the spin magnetic moments around the horizontal x-axis in the hypothetical 'single-electron $BiCoO_3$' (similar bunching exists in $PbVO_3$ – Fig. 4, but the effect is considerably weaker). Second, the easy-axis alignment in $BiCoO_3$ is solely related to the single-ion anisotropy term: as long as it is absent in the hypothetical 'single-electron $BiCoO_3$', the spin magnetic moments start to regroup around the x-axis.

Finally, we comment on the dependence of our results on different levels of treatment of the relativistic SOI. We consider two such schemes: (i) the SOI was included to the model Hamiltonian as a pseudo-perturbation only at the transition-metal sites,[10] and (ii) the SOI was included at all sites of the system (including heavy Pb and Bi elements) in the process of downfolding procedure. However, the distribution of the spin magnetic moments, obtained in these two schemes, is practically indistinguishable (Fig. 7). Thus, the SOI at the heavy Pb- and Bi-elements does not seem to play an important role in the magnetic properties of

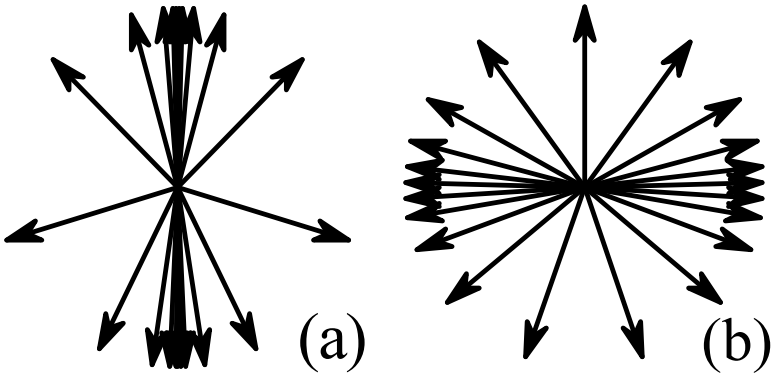

FIG. 6. Distribution of the spin magnetic moments (as if they were brought to the same origin), obtained in the Hartree-Fock calculations for L= 21. Left panel (a) shows results for the regular $BiCoO_3$, involving six valence electrons. Right panel (b) shows the same results for the hypothetical system, which has the same parameters of electronic Hamiltonian as for $BiCoO_3$ and only one valence electron. Thus, according to the Kramers theorem, the single-ion anisotropy terms should not operate in the case (b). Here, x is the horizontal axis and z is the vertical one.

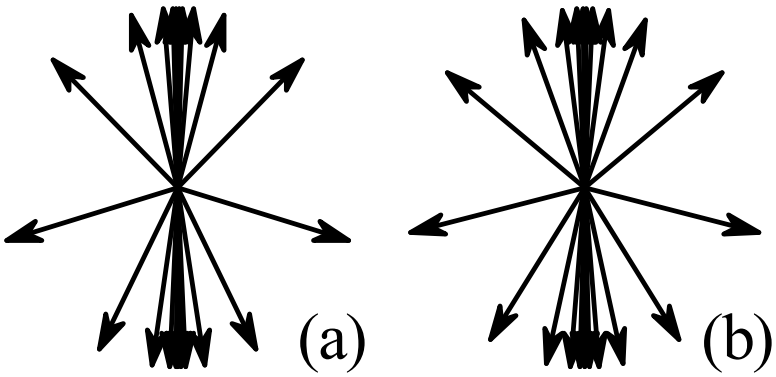

FIG. 7. Influence of the spin-orbit interaction on the magnetic structure of $BiCoO_3$ (results for L= 21). Left panel (a) shows the results, where the spin-orbit interaction was included only on the Co-sites. Right panel (b) shows the results, where the spin-orbit interaction was included on all sites of the system, through the downfolding procedure. Here, x is the horizontal axis and z is the vertical one.

$PbVO_3$ and $BiCoO_3$.

IV. CONCLUSIONS

Being based on results of the low-energy electronic model, derived from the first-principles electronic structure calculations, we analyzed possible magnetic structures of two noncentrosymmetric perovskites $PbVO_3$ and $BiCoO_3$. We have argued that, despite structural similarities, the magnetic behavior of these two materials is expected to be very different. $PbVO_3$, with the spin $S = 1/2$, should form a long-periodic spin-spiral state, which results solely from the competition between isotropic exchange and Dzyaloshinskii-Moriya interactions in the noncentrosymmetric crystal structure. Due to the Kramers degeneracy, the single-ion anisotropy does not operated in $PbVO_3$. However, the latter is expected to play a major role in $BiCoO_3$, which has the spin $S = 2$. Particularly, the single-ion anisotropy suppress the noncollinear spin-spiral alignment in $BiCoO_3$ and enforces the formation of the C-type antiferromagnetic ground state, in agreement with the experiment.[3]

We believe that this funding has a direct implication to the properties multiferroic manganites, which also have spin $S = 2$ and the large single-ion anisotropy.[15] Therefore, the numerous claims about the spin-spiral ground state of these compounds, and related to it improper ferroelectric activity, should be taken cautiously. Again, due to the large single-ion anisotropy, the ground state of manganites is not necessary the spin spiral, which prompts a search for alternative mechanism of multiferroicity in these compounds.[12]

---

* SOLOVYEV.Igor@nims.go.jp

[1] D. Lebeugle, D. Colson, A. Forget, M. Viret, A. M. Batailee, and A. Gukasov, Phys. Rev. Lett. **100**, 227602 (2008).

[2] A. A. Belik, M. Azuma, T. Saito, Y. Shimakawa, and M. Takano, Chem. Mater. **17**, 269 (2005).

[3] A. A. Belik, S. Iikubo, K. Kodama, N. Igawa, S.-I. Shamoto, S. Niitaka, M. Azuma, Y. Shimakawa, M. Takano, F. Izumi, and E. Takayama-Muromachi, Chem. Mater. **18**, 798 (2006).

[4] R. V. Shpanchenko, V. V. Chernaya, A. A. Tsirlin, P. S. Chizhov, D. E. Sklovsky, E. V. Antipov, E. P. Khlybov, V. Pomjakushin, A. M. Balagurov, J. E. Medvedeva, E. E. Kaul, and C. Geibel, Chem. Mater. **16**, 3267 (2004).

[5] A. A. Tsirlin, A. B. Belik, R. V. Shpanchenko, E. V. Antipov, E. Takayama-Muromachi, and H. Rosner, Phys. Rev. B **77**, 092402 (2008).

[6] Y. Uratani, T. Shishidou, F. Ishii, and T. Oguchi, Japanese Journal of Applied Physics **44**, 7130 (2005).

[7] D. J. Singh, Phys. Rev. B **73**, 094102 (2006).

[8] I. Dzyaloshinsky, J. Chem. Phys. Solids **4**, 241 (1958); T. Moriya, Phys. Rev. **120**, 91 (1960).

[9] H. Katsura, N. Nagaosa, and A. V. Balatsky, Phys. Rev. Lett. **95**, 057205 (2005); M. Mostovoy, Phys. Rev. Lett. **96**, 067601 (2006); I. A. Sergienko and E. Dagotto, Phys. Rev. B **73**, 094434 (2006).

[10] I. V. Solovyev, J. Phys.: Condens. Matter **20**, 293201 (2008).

[11] I. V. Solovyev and Z. V. Pchelkina, Phys. Rev. B **82**, 094425 (2010).

[12] I. V. Solovyev, Phys. Rev. B **83**, 054404 (2011).

[13] Supplemental materials.

[14] I. Sosnowska and A. K. Zvezdin, J. Magn. Magn. Mater. **140-144**, 167 (1995).

[15] I. Solovyev, N. Hamada, and K. Terakura, Phys. Rev. Lett. **76**, 4825 (1996).

[16] I. V. Solovyev, New J. Phys. **11**, 093003 (2009).

[17] A. Kumar, L. W. Martin, S. Denev, J. B. Kortright, Y. Suzuki, R. Ramesh, and V. Gopalan, Phys. Rev. B **75**, 060101(R) (2007).

[18] W. C. Koehler, J. W. Cable, M. K. Wilkinson, and E. O. Wollan, Phys. Rev. **151**, 414 (1966); G. P. Felcher, G. H. Lander, T. Arai, S. K. Sinha, and F. H. Spedding, Phys. Rev. B **13**, 3034 (1976).